Nomenclature

$\Lambda_{12}, \Lambda_{21}$ = Wilson parameters
B_{ii} = pure component second virial coefficient, cm^3/mol
B_{ij} = second virial cross coefficient, cm^3/mol
D = Herington's parameter
$f^{(0)}, f^{(1)}$ = dimensionless terms in Equation 3 of Tsonopoulos
J = Herington's parameter
P = total pressure, atm
P_i^s = saturated vapor pressure of pure component i, atm
P_{ci} = critical pressure of i, atm
R = gas constant, cm^3-atm/deg-mol
T = temperature, K
T_{ci} = critical temperature of i, K
T_R = reduced temperature
V_i^L = liquid molar volume of i, cm^3/mol
x_i = liquid molar composition
y_i = vapor molar composition

Greek Letters

γ_i = liquid-phase activity coefficient of component i
θ = range of boiling points of systems, °C
$\lambda_{12} - \lambda_{11}$ = energy parameters of Wilson equation, cal/mol
$\lambda_{12} - \lambda_{22}$ = energy parameters of Wilson equation, cal/mol
ω_i = acentric factor of component i

Subscripts

1, 2 = 1: cyclohexane in first system and 2,4-DMP in second
system; 2: TBA in both cases

Literature Cited

(1) Dreisbach, R. R., *Advan. Chem. Ser.*, **15, 22**, American Chemical Society, Washington, D.C., 1955, 1959.
(2) Fowler, R. T., Norris, G. S., *J. Appl. Chem. (London)*, **5**, 266 (1955).
(3) Hala, E., Pick, J., Fried, V., Vilim, O., "Vapor-Liquid Equilibrium," Pergamon, London, England, 1967.
(4) Hala, E., Wichterle, I., Polak, J., Boublik, T., "Vapor-Liquid Equilibrium at Atmospheric Pressures," Pergamon, London, England, 1968.
(5) Herington, E.C.G., *J. Inst. Petrol.*, **37**, 457 (1951).
(6) Horsley, L. H., "Azeotropic Data," American Chemical Society, Washington, D.C., 1952.
(7) Pitzer, K. S., Curl, R. F., *J. Am. Chem. Soc.*, **79**, 2369 (1957).
(8) Prausnitz, J. M., "Molecular Thermodynamics of Fluid Phase Equilibria," p 204, Prentice-Hall, Englewood Cliffs, N.J., 1969.
(9) Prausnitz, J. M., Eckert, C. A., Orye, R. V., O'Connell, J. P., "Computer Calculations of Multicomponent Vapor-Liquid Equilibria," Prentice-Hall, Englewood Cliffs, N.J., 1967.
(10) Rao, C.N.R., George, M. V., Mahanty, J., Narasimahan, P. T., "A Handbook of Chemistry and Physics," Affiliated East-West Press, New Delhi, India, 1967.
(11) Redlich, O., Kister, A. T., *Ind. Eng. Chem.*, **40**, 341 (1948).
(12) Reid, R. C., Sherwood, T. K., "Properties of Gases and Liquids," McGraw-Hill, New York, N.Y., 1958.
(13) "Technical Data Book—Petroleum Refining," American Petroleum Institute, Division of Refining, New York, N.Y., 1966.
(14) Tripathi, R. P., Sagar, J. M., Gulati, I. B., *J. Appl. Chem. Biotechnol.*, **23**, 681 (1973).
(15) Tsonopoulos, C., *AIChE J.*, **20** (2), 263 (1974).
(16) Van Ness, H. C., "Classical Thermodynamics of Non-Electrolyte Solutions," p 136, Macmillan, New York, N.Y., 1964.
(17) Weast, R. C., "Handbook of Chemistry and Physics," 50th ed., Chemical Rubber Co., Cleveland, Ohio, 1969.
(18) Wilson, G. M., *J. Am. Chem. Soc.*, **86**, 127 (1964).
(19) Wohl, K., *Trans. Am. Inst. Chem. Eng.*, **42**, 215 (1946).
(20) Yen, L. C., Woods, S. S., *AIChE J.*, **12** (1), 95 (1968).

High-Temperature Solubilities of Calcium Sulfate Hemihydrate and Anhydrite in Natural Seawater Concentrates

Julius Glater[1] and John Schwartz[2]
School of Engineering and Applied Science, University of California, Los Angeles, Calif. 90024

Solubilities of the high-temperature calcium sulfate modifications, hemihydrate and anhydrite, are measured in natural seawater at temperatures up to 165°C. Scaling thresholds or concentration-temperature limits are determined over a temperature range of 91–162°C. A new graphical method of scaling threshold evaluation is described. Experimental data presented here are compared with literature values. Scaling thresholds calculated from the extended Debye-Hückel theory are in good agreement with the experimental results. A complete scaling threshold diagram for hemihydrate and anhydrite is also developed. Scaling threshold evaluation is important in the operation of desalting equipment, boilers, and cooling towers.

Understanding the solution chemistry of high-temperature calcium sulfate modifications is vitally important to the design and operation of saline water evaporators. Both hemihydrate and anhydrite scale may deposit by concentrating natural wa-

ters at temperatures above the ambient boiling point. The resultant scale composition cannot be predicted solely from solubility considerations but also depends on rates of transformation of metastable hemihydrate to anhydrite, the stable phase. The goal of modern distillation technology is directed toward increasing brine concentrations and/or operating temperatures so that lower product water costs can be achieved.

Nature has apparently contrived a system which opposes either of these tendencies because of potential scaling. First, solutions are brought closer to saturation as concentration increases. Second, the solubilities of both hemihydrate and anhydrite fall off rapidly with increasing temperature. Third, the rate of conversion of hemihydrate to anhydrite is accelerated at higher temperatures and brine concentrations. The third phenomenon severely limits evaporator residence time since anhydrite is so insoluble that practical evaporation cannot be achieved under conditions where this scale form is expected.

A most effective tool for prediction of scaling conditions is the scaling threshold diagram described by Glater and Fung (5) and Glater (3) and commonly referred to in the literature as a solubility diagram. Scaling thresholds represent a match of temperature and brine concentration corresponding to

---

[1] To whom correspondence should be addressed.
[2] Present address, School of Medicine, St. Louis University, St. Louis, Mo.

equilibrium between solid and dissolved salt in a particular water sample. Thresholds may also be defined as the maximum permissible concentration factor at fixed temperature or the maximum permissible temperature at fixed concentration factor required to induce scale nucleation under equilibrium conditions.

Scaling thresholds provide boundary conditions based on chemical equilibrium alone. This criterion is generally satisfactory for establishing distillation parameters, but excessive heat transfer rates or tendency toward supersaturation may lower or raise the operational scaling threshold, respectively. Work described in this paper is based on equilibrium conditions only and will not take into account other factors.

Scaling thresholds may be evaluated directly by heating a water sample at constant concentration or evaporating at constant temperature until incipient crystallization is observed in transparent apparatus. Visual methods described by Glater et al. (7) and Glater (3) are simple, rapid, and fairly reproducible, but some error may result from a slight tendency toward supersaturation, in spite of good agitation. Calculation methods based on the Debye-Hückel theory have been published by Marshall and Slusher (12), Lu and Fabuss (10), and recently by Filippov et al. (2). These methods require accurate water analysis, and results do not always agree with experimental data due to limitations of the Debye-Hückel theory in concentrated electrolyte solutions.

The most reliable scaling threshold values are obtained experimentally from solubility measurements in natural water concentrates. Few experimental studies of this kind have been conducted in natural seawater at temperatures above the ambient boiling point. Data on hemihydrate are especially sparse because of difficulties in working with this metastable compound. This is unfortunate since hemihydrate is the scale modification anticipated in the usual range of distilling temperatures. Prior to this work, the only experimental studies in natural seawater were reported in the early 1930's by Toriumi et al. (18). Additionally, some experimental data in synthetic seawater have been published by Lu and Fabuss (10) and Marshall and Slusher (12).

At this point we will distinguish between the often confused terms solubility and scaling threshold. Solubility is a measure of the salt concentration in a saturated solution at constant temperature and ionic background. Scaling threshold, on the other hand, takes into consideration the effects of both changing background and temperature on solubility. During the evaporation of a natural water, we proceed to change the concentration factor (CF) or temperature or both. By altering these parameters sufficiently, nucleation of some scaling compound will ultimately begin. This critical match of conditions is defined as the scaling threshold. Since solubility is a complex function of both temperature and concentration factors, measurements under one set of conditions cannot be simply extrapolated to another set of conditions.

For example, in saline water evaporation we start with an unsaturated solution of some scaling compound. During evaporation the scaling compound is brought closer to saturation, but, simultaneously, dissolved background salts such as sodium chloride are also increasing in concentration. Since solubility of the scaling compound varies with background concentration, its value is constantly changing as evaporation continues. At the scaling threshold, the compound's ion product must equal its solubility product at the particular ionic strength. This equality may be determined by measuring a series of solubility products at different background concentration levels and calculating the ion product for each level. The scaling threshold can then be evaluated by plotting solubility products along with ion products on the same graph and determining the intersection of these two lines. By definition, equilibrium conditions are satisfied when the ion product, IP,

equals the solubility product, K_{sp}. The solution is saturated at conditions represented by this intersection point. Graphical methods were first described by Posnjak (15), later refined by Langelier et al. (9), and further modified in the work described here.

This paper presents new measurements of calcium sulfate solubility in natural seawater. Experimental methods for scaling threshold evaluation are also discussed. A complete scaling threshold diagram for hemihydrate and anhydrite has been developed, and results are compared with experimental and theoretical work of other investigators.

Apparatus and Experimental Procedure

This experimental study involves measurements of equilibrium solubilities of calcium sulfate hemihydrate and anhydrite at temperatures above 212°F. To meet this requirement it was necessary to design a pressure vessel chemically inert to seawater brines and capable of withstanding temperatures up to 400°F and pressures in the order of 150 psig and to provide instrumentation for constant temperature control and accurate temperature measurement.

The final hydrothermal equipment was built quite inexpensively from standard component parts. The pressure vessel shown in Figure 1 is a standard stainless-steel Parr bomb (Parr Instruments, No. 4760) of 310-ml capacity. The vessel was supplied with a blank head modified to accommodate a thermocouple port for measuring solution temperature, a thermistor port to drive the temperature control unit, and a sample port for removing internally filtered solutions. The sample port was designed so that fine fritted glass filter sticks could be easily exchanged for cleaning. A pressure gauge, gas pressurization port, and necessary valves were also provided in the final assembly. Thermocouple and thermistor wells were fabricated from stainless-steel tubing and bolted into the pressure vessel head. All interior surfaces in contact with liquids, including thermocouple and thermistor wells, were coated with a special heat-cured Teflon spray. This coating was applied to ensure inertness toward hot concentrated salt solutions. The coating provided by Drilube Inc., Glendale, Calif., showed good durability at temperatures up to approximately 400°F.

The pressure vessel assembly was heated in a standard glass-col heating mantle designed for 1-l. beakers. Power was supplied through a combined magnetic stirrer, hot plate, temperature controller assembly (Cole-Parmer Model 4812). This unit was modified by disconnecting the hot plate leads and wiring the heating mantle directly to the temperature control output. Consequently, the hot plate was bypassed by use of the Cole-Parmer unit for magnetic stirring and temperature control only. Greater thermal stability was achieved by wrapping the upper exposed portion of the pressure vessel with in-
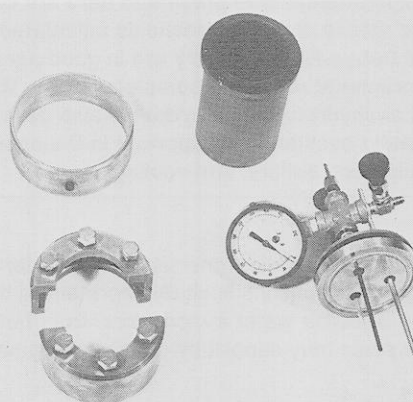

Figure 1. Details of pressure vessel assembly

sulating asbestos tape. With this assembly, operating temperatures between 212° and 400°F could be achieved within 25–35 min from room temperature. Temperature control was effected to within plus or minus 1°F of the desired operating temperature. Accurate temperature measurements were carried out with a copper constantan thermocouple with a Leeds-Northrup potentiometer Model 8690. The complete hydrothermal apparatus assembly, including sample condenser, is shown in Figure 2.

All scaling thresholds were determined in natural seawater concentrates over a temperature range between 212° and 340°F. Natural seawater from Marineland, Calif., was selected for this study because of its clarity and constancy of composition. Routine calcium and magnesium analysis over a period of years gave average values of 393 and 1297 ppm, respectively, and showed insignificant variation with tide, sea temperature, or season. Average values are in good agreement with "normal seawater" prepared by the Hydrographic Laboratories at Copenhagen, Denmark.

Seawater concentrates for hemihydrate equilibration studies were saturated with calcium sulfate and prepared as follows. A 10-l. sample of Marineland seawater was acidified to pH 4.0 with hydrochloric acid to decompose bicarbonate ion, thus preventing the formation of alkaline scale. The sample was then evaporated slowly without spattering to a volume of 2.5 l. corresponding to CF 4.0. Samples of lower concentration factor were prepared from this concentrated stock solution by dilution with distilled water to the desired CF value. The concentration factor was calculated from the relationship $CF = V_i/V_f$, where V_i and V_f are initial and final solution volumes, respectively. Each concentrate was now saturated with calcium sulfate at ambient temperature by stirring with reagent grade gypsum for 4 hr. The resulting slurries were allowed to stand overnight and then filtered through fine fritted glass.

Hemihydrate solubility in each concentrate was measured by transferring a 200-ml aliquot of saturated solution to the pressure vessel. The pressure vessel head was clamped into position, and the system pressurized to about 10 psig with compressed nitrogen to prevent boiling during initial heating. The assembled pressure vessel was placed in the heating mantle, fitted with thermistor and thermocouple probes, and heated at maximum rate to the desired experimental temperature. The system was maintained at constant temperature ±1°F and magnetically stirred throughout the experimental period. Times of equilibration were chosen in accordance with the experimental temperature. The basis for selection of appropriate times will be discussed in the Results and Discussion section.

At the completion of an experimental run, 3-ml samples were withdrawn for calcium analysis through the fine internal fritted glass filter stick connected to a water cooled condenser. Sample flow was activated through positive pressure within the system. Analyses were performed by atomic absorption spectrophotometry using standard techniques. A Perkin-Elmer Model 303 instrument was used for all analyses.

The identity of certain solid samples was verified by X-ray diffraction analysis. This was accomplished by cooling the pressure vessel rapidly in ice after equilibrium was clearly established. Solids were separated by filtration and washing with distilled water followed by acetone.

Anhydrite solubility in seawater concentrates was determined in the same manner as hemihydrate with the exception that samples were not saturated with gypsum. Instead, approximately 1 g of reagent grade anhydrite was added directly to each 200-ml water sample in the pressure vessel. All other aspects of the experimental procedure were the same except that longer times were required to establish equilibrium with anhydrite.
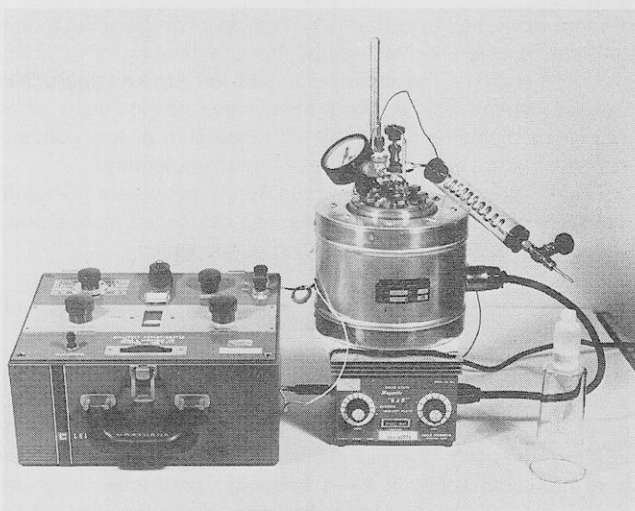

Figure 2. Assembled hydrothermal equipment with thermocouple potentiometer

Results and Discussion

Hemihydrate equilibria. The calcium sulfate phase diagram in distilled water, published by Partridge and White (14), shows three distinct crystal modifications in equilibrium with aqueous solutions. At room temperature, gypsum is the stable modification, undergoing phase transition to hemihydrate at 98°C. At this temperature both forms have the same solubility, but solid $CaSO_4 \cdot 2H_2O$ undergoes rapid dehydration to $CaSO_4 \cdot \frac{1}{2}H_2O$. Bock (1) has shown that phase transition temperatures are shifted to lower levels as background salinity is increased, but even in seawater concentrates, transition occurs near the ambient boiling point.

Gypsum saturated seawater solutions at room temperature deposit solid hemihydrate in a matter of minutes at temperatures above the ambient boiling point. Because of hemihydrate's inverted solubility, the amount of solid increases with increasing temperature. At temperatures near 212°F, equilibrium with hemihydrate is established within 15 min as indicated by constant levels of dissolved calcium ion. Attainment of equilibrium becomes even faster as the temperature increases.

Calcium sulfate hemihydrate can be generated in situ and equilibrated readily with seawater concentrates above 98°C. An important consideration in this system, however, is the lifetime of the resulting metastable hemihydrate phase. Langelier et al. (9) first observed that hemihydrate is stable in CF 1 seawater for approximately 17 hr at 212°F. The mechanism of this delayed reaction is not understood, but phase transition rates have been studied by Johnson (8), Murdia et al. (13), and recently by Glater and Dooly (4). All of these studies show the lifetime of hemihydrate to decrease exponentially with increasing temperature. The 17-hr metastability at 212°F is diminished to approximately 15 min at 340°F. This was considered the maximum working temperature for these experiments. At temperatures above this level, transition to hemihydrate takes place so rapidly that solubility cannot be evaluated by equilibration methods. Special care was thus taken throughout this work to ensure equilibrium with pure hemihydrate since mixtures with anhydrite could result from long equilibration periods. This problem was especially critical at high temperatures. Equilibrium was always verified by constancy of calcium concentration and by X-ray diffraction of selected solid samples.

Scaling thresholds were first evaluated according to the graphical procedure described by Langelier et al. (9). In the

present work, however, the negative log of calcium ion molality (pCa^{+2}) was used instead of the negative log of solubility product (pK_{sp}) or the negative log of ion product (pIP). The levels of sulfate ion concentration were not included since they are stoichiometrically related to calcium at any concentration and consequently will not vary independently.

Table I presents solubility data for hemihydrate. Calcium molality (m) in saturated solutions was calculated from atomic absorption readout by the following relationship:

$$m = \frac{C}{40.08\,[\rho - (36.047 \times CF)]} \times 200 \tag{1}$$

In this equation, C is AA readout in milligrams Ca^{+2} per liter, ρ is density in grams per liter, and CF is concentration factor on a volumetric basis. The ionic weight of calcium is 40.08, 200 represents a sample dilution factor, and 36.047 is the total dissolved solids in CF 1 seawater expressed in grams per liter. No correction was made for the density of diluted samples which were assumed to equal 1.00 g/ml.

Table II presents calculated calcium molalities as a function of concentration factor. Marineland seawater of CF 1 had an average calcium concentration of 393 ppm. Calcium molalities (m) in concentrated and diluted seawater (unsaturated solutions) were calculated as follows:

$$m = \frac{C_1}{\left[1000 - \left(35.175 \times CF \times \frac{\rho_1}{\rho_2}\right)\right] 40.08} \tag{2}$$

In this equation C_1 is the calcium concentration in ppm, and 35.175 is the total dissolved solids in CF 1 seawater expressed in grams per kilogram, ρ_1 and ρ_2 are densities of CF 1 seawater and seawater at the other CF, respectively.

Figure 3 represents a typical Langelier-type plot for two different experimental temperatures. The line sloping down to the right is a plot of calculated values for pCa^{+2} taken from Table II. The two curved horizontal lines are plots of pCa^{+2} values in saturated solutions taken from solubility measurements at the specified temperatures. Intersections correspond to hemihydrate scaling thresholds at 245° and 275°F. This graphical process was repeated at several other temperature levels to generate the scaling threshold data presented in Table III.

During the course of this work, a new experimental and graphical method was developed. By this method the CF is maintained constant, and solubilities are measured at a series of temperatures on the same seawater sample. The new technique, illustrated in Figure 4, shows a plot of pCa^{+2} vs. temperature. The horizontal line represents constant calcium molality at the fixed concentration factor of one. The line sloping up to the right is a plot of solubility values as a function of temperature at this fixed CF. Each data point represents equilibrium with solid hemihydrate for the specific temperature. Points below and above the horizontal line contain higher and lower calcium ion concentrations, respectively, than are present in CF 1 seawater. At the intersection, the equilibrium calcium concentration is equal to that present in CF 1 seawater. This point, the hemihydrate scaling threshold, corresponds to 324°F in CF 1 seawater.

Another way of looking at this diagram is to consider points along the horizontal line. Those points to the right of the intersection represent supersaturation, and those to the left are unsaturated. If acidified CF 1 water is heated without further treatment or concentration, hemihydrate will just begin precipitation at 324°F.

This new graphical method has several advantages over the Langelier technique. First, the line intersections are sharper since both lines are nearly straight. Second, it is possible to extend scaling threshold evaluation to higher and lower tem-

Table I. Typical Hemihydrate Solubilities in Seawater Concentrates

CF	ρ, g/l. at 25°C	Temp, °F	AA readout,[a] ppm	Ca^{+2} molality $\times 10^2$	$-\log Ca^{+2}$ molality
1.00	1024	295.5	2.56	1.292	1.889
		315.0	2.24	1.131	1.947
		322.0	2.04	1.026	1.987
		329.0	1.92	0.969	2.014
1.80	1044	275.0	3.88	1.977	1.704
		287.5	3.40	1.733	1.761
		295.5	3.20	1.631	1.788
2.00	1048	247.0	4.97	2.541	1.595
		262.5	4.50	2.301	1.638
		275.0	4.04	2.066	1.685
		287.5	3.47	1.774	1.751
2.50	1061	230.0	5.96	3.063	1.514
		247.0	5.15	2.647	1.577
		262.5	4.70	2.401	1.620
		275.0	4.16	2.132	1.671
3.00	1073	217.0	6.18	3.196	1.495
		227.5	5.80	2.999	1.523
		238.0	5.32	2.751	1.561
		250.0	4.75	2.456	1.610
3.40	1083	216.5	6.07	3.153	1.501
		227.0	5.74	2.982	1.526
		238.0	5.27	2.738	1.562
		247.0	4.63	2.405	1.619

[a] All samples were diluted by a factor of 200×. In diluted solutions, AA readout in ppm was assumed to equal mg/l. since density is very close to 1000 g/kg.

Table II. Calcium Ion Concentration in Diluted and Concentrated Seawater at 25°C

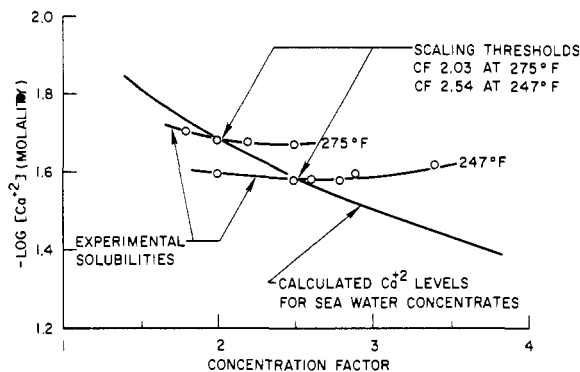| CF	ρ, g/l. at 25°C	ppm Ca^{+2}	Ca^{+2} molality $\times 10^2$	$-\log Ca^{+2}$ molality
0.25	1000	100	0.252	2.599
0.50	1010	199	0.506	2.296
0.75	1017	301	0.772	2.113
1.00	1024	393	1.016	1.993
1.20	1028	469	1.222	1.913
1.50	1036	582	1.532	1.815
2.00	1048	767	2.055	1.687
2.50	1061	947	2.582	1.588
3.00	1072	1124	3.119	1.506
3.50	1084	1300	3.671	1.435

Figure 3. Hemihydrate scaling threshold determination in seawater at 247° and 275°F according to Langelier method

peratures by extrapolation of the solubility line. Third, the experimental technique is much simpler since several data points can be generated from a single solution at a fixed concentration factor by variation of temperature.

Anhydrite equilibria. Anhydrite solubilities and scaling thresholds were determined in a similar manner to hemihydrate, with a few experimental differences. Since anhydrite is the stable modification over the entire temperature range, equilibration could be continued for indefinite time intervals. Much longer periods of time were required to establish equilibrium with anhydrite. Equilibration periods were inversely related to temperature and salinity. They varied roughly between 14 hr at 240°F and 7 hr at 340°F. Experiments were performed by first heating a saturated solution to its maximum operating temperature for a given experimental run. In the case of CF 1 water, this was 260°F. Equilibration times were then determined by following the decrease in calcium concentration with time from the resulting supersaturated solutions. The process was repeated at each succeeding lower temperature.

Because of the lower solubility of anhydrite, it became necessary to equilibrate certain samples in dilute seawater below CF 1. Figure 5 shows a typical scaling threshold intersection in CF 0.50 seawater. Anhydrite solubilities in molal units were calculated in the manner described in the preceding section. Scaling threshold data for anhydrite are summarized in Table IV.

Summary of calcium sulfate scaling thresholds. Figure 6 represents a CF-temperature plot of hemihydrate and anhydrite scaling thresholds derived from this work compared with other literature values. The two other experimental lines on the diagram (one for hemihydrate and one for anhydrite) were

determined graphically from the solubility data of Toriumi et al. (18) and Tanaka et al. (17), respectively. Scaling thresholds were evaluated from Langelier-type plots of solubility data reported in these papers. Agreement between the present work and results from the Japanese papers published in the 1930's is truly remarkable, considering the widely differing analytical methods used for solubility determination. In the Japanese experiments, dissolved calcium sulfate was measured by light interferometry as compared with atomic absorption spectrophotometry used in this study.

The lowest line in the hemihydrate family of curves was drawn from limited data taken from actual distilling plants by Standiford and Sinek (16). There is considerable uncertainty in the position of this line because of the difficulty in relating an exact CF level with the onset of scaling. In addition, the identity of solid phases was not clearly established in this work.

The other two lines in each series were calculated from thermodynamic K_{sp} values using the extended Debye-Hückel theory with added terms. All data used for computation by Lu and Fabuss (10) were obtained from the literature. The line labeled Lu and Fabuss in Figure 6 was taken directly from their published graph. The computation scheme presented by Marshall and Slusher (12), however, was verified by these investigators experimentally in synthetic seawater. Deviation from the Debye-Hückel theory was assumed to result from complexing of sulfate by magnesium ion. K_d values for the resulting $MgSO_4^0$ ion pair were also determined experimentally by Marshall (11) and used in a computer program designed to read out temperature-CF matches for all three calcium sulfate modifications. The line labeled Marshall and Slusher in Figure 6 was calculated by the computer program using con-

Table III. Hemihydrate Scaling Threshold Limits for Seawater

Temp, °F	CF
196.0	3.40
224.0	3.00
230.0	2.89
247.0	2.54
262.5	2.28
275.0	2.03
287.5	1.67
295.5	1.47
311.0	1.20
324.0	1.00

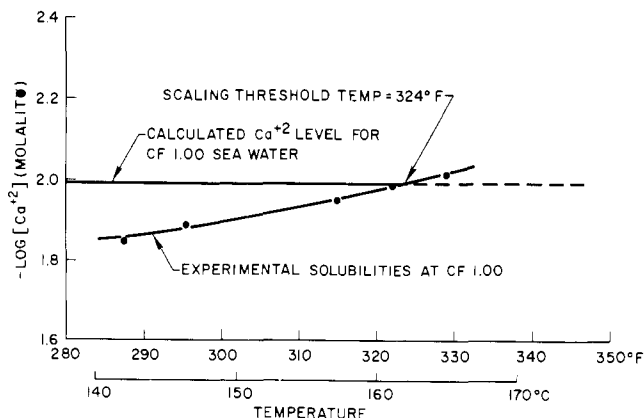Figure 5. Anhydrite scaling threshold determination in seawater at constant concentration factor of 0.50
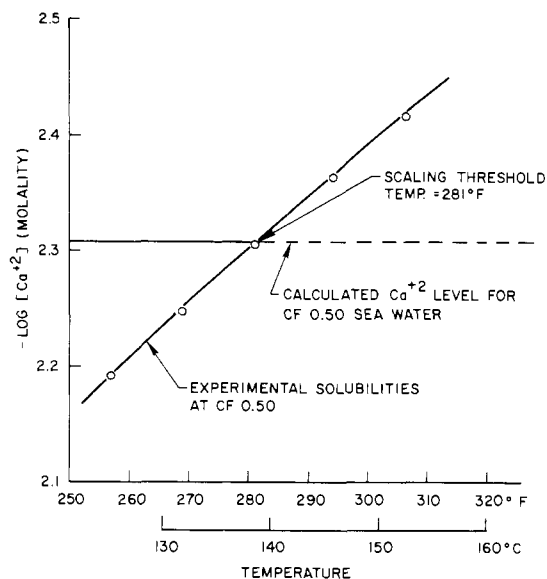

Figure 4. Hemihydrate scaling threshold determination in seawater at constant concentration factor of 1.00

Table IV. Anhydrite Scaling Threshold Limits for Seawater

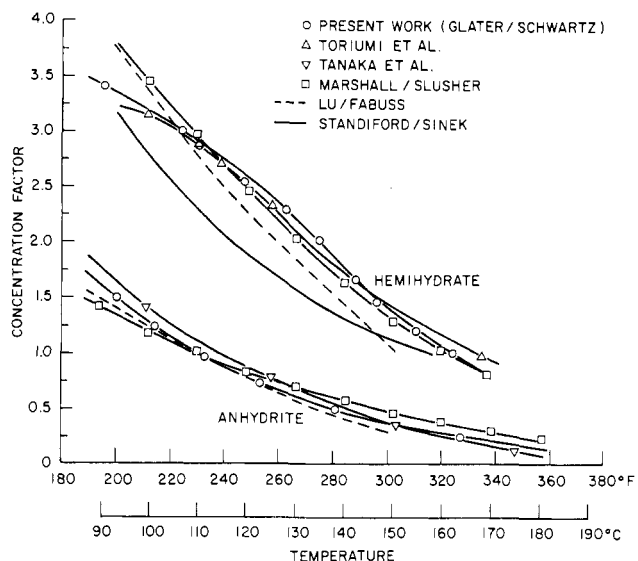| Temp, °F	CF
200	1.50
214	1.25
232	1.00
253	0.75
281	0.50
292	0.25

Figure 6. Scaling thresholds of hemihydrate and anhydrite in seawater compared with experimental and calculated values from literature

centrations of calcium and magnesium ions measured in Marineland seawater and a total ionic strength of $0.7229m$, corresponding to standard seawater.

Excellent agreement between experimental data from this work and that reported in the Marshall-Slusher computer program is evident from Figure 6. The Marshall-Slusher program has, in fact, proved successful for scaling threshold prediction in most natural waters of normal ionic distribution. One weakness of this calculation method, however, is the high value for hemihydrate near the ambient boiling point. Glater et al. (6) also observed that overall low values for hemihydrate are derived from the computer program in solutions containing high levels of magnesium ion.

Figure 6 presents a summary of the best available data on scaling thresholds of high-temperature calcium sulfate modifications. Seawater distillation above the ambient boiling point would be virtually impossible if anhydrite were the dominant scale form since saturation is achieved in CF 1 water at about 232°F. Fortunately, this is not the case. Although anhydrite is the stable high-temperature modification, hemihydrate remains metastable for considerable time periods in the usual range of distilling temperatures. For example, at 250°F the transition time between these forms is approximately 3 hr in CF 2 seawater. This is much longer than average brine retention time in conventional evaporators. Seawater distilling plants are therefore designed to operate at conditions above the anhydrite line but below the line for hemihydrate.

Conclusions

Solubilities of calcium sulfate hemihydrate and anhydrite have been measured in natural seawater over the tempera-

ture range of 212° to 329°F and at concentration factors between 0.25 and 3.50. Boundary conditions for precipitation of these scale modifications were evaluated from experimental data. The evaluation was carried out by a new graphical method described in this paper. Experimentally derived scaling thresholds are generally in good agreement with values calculated by the Marshall-Slusher computer program (12).

The scaling threshold diagram presented in this paper should be useful for establishment of design and operating limits in seawater distilling plants. It is important to remember, however, that true equilibrium conditions are rarely encountered in the field. For example, bulk brine temperature cannot be used directly for scaling threshold prediction since temperatures near the heat transfer surface are always higher. Threshold diagrams can thus be used to set maximum distilling parameters which may have to be modified downward to some extent for a particular evaporator. Variation from equilibrium boundary conditions will depend on brine velocity, fluid dynamics, heat transfer rate, and heat transfer surface conditions.

Literature Cited

(1) Bock, E., Can. J. Chem., **39**, 1746 (1961).
(2) Filippov, S. N., Kolotigin, Y. A., Ovchinikov, S. A., Proc. 4th International Symposium on Fresh Water from the Sea, Vol 2, pp 111–117, Heidelberg, West Germany, September 1973.
(3) Glater, J., Chem. Eng. Progr. Tech. Manual, T40, Cooling Towers, pp 138–45, 1972.
(4) Glater, J., Dooly, R., University of California Water Resources Center Desalination Report No. 57, 1974.
(5) Glater, J., Fung, K., Environ. Sci. Technol., **3**, 580 (1969).
(6) Glater, J., Murdia, K. S., Dooly, R., Desalination, **14**, 197 (1974).
(7) Glater, J., Ssutu, L., McCutchan, J. W., Environ. Sci. Technol., **1**, 41 (1967).
(8) Johnson, D. R., PhD dissertation, Dept. Chem. Met. Eng., Univ. Michigan, Ann Arbor, Mich., 1967.
(9) Langelier, W. F., Caldwell, D. H., Lawrence, W. B., Ind. Eng. Chem., **42**, 126 (1950).
(10) Lu, C. H., Fabuss, B. M., Ind. Eng. Chem., Process Des. Dev., **7**, 206 (1968).
(11) Marshall, W. L., J. Phys. Chem., **71**, 3584 (1967).
(12) Marshall, W. L., Slusher, R., J. Chem. Eng. Data, **13**, 83 (1968).
(13) Murdia, K., Glater, J., McCutchan, J. W., Univ. California, Los Angeles, UCLA-ENG-7232, Water Resources Center Desalination Report No. 49, 1972.
(14) Partridge, E. P., White, A. H., J. Am. Chem. Soc., **51**, 360 (1929).
(15) Posnjak, E., Am. J. Sci., **238**, 559 (1940).
(16) Standiford, F. C., Sinek, J. R., Chem. Eng. Progr., **57**, 58 (1961).
(17) Tanaka, Y., Nakamura, K., Hara, R., Kogyo Kagaku Zasshi, **34**, 779 (1931).
(18) Toriumi, T., Kuwahara, T., Hara, R., ibid., **36**, 1651 (1933).